Experimental Study of the Nonlinear Dynamics of an Actively Q-Switched Ytterbium-Doped Fiber Laser

Yuri O. Barmenkov, *Member, IEEE*, Alexander V. Kir'yanov, *Member, IEEE*, and Miguel V. Andrés, *Member, IEEE*

***Abstract*— In this paper, a comprehensive experimental study of the dynamics of an actively Q-switched Yb-doped GTWave-based fiber laser is presented. It is shown that the appearance of the Q-switching regime in the laser is sensitive to both the repetition rate and the temporal width of the transparency window of an acousto-optical Q-switch modulator placed in the cavity. It is also shown that, at low repetition rates, a peculiar self-Q-switch regime induced by stimulated Brillouin scattering is observed in the laser, which interferes stochastically with the regular (true) active Q-switching mode. While increasing the Q-modulator repetition rate, the self-Q-switch pulsing steadily vanishes but the true Q-switching remains. The latter, however, becomes strongly subjected, while further increasing the Q-switch repetition rate, by the nonlinear laser dynamics effects. That is, the laser is allowed to operate at certain subharmonics of the repetition rate or in some specific regimes that occur at laser transients from one attractor to another. These transient regimes are characterized by alternating between pulse amplitude and energy, and pulse spacing or chaos, which is strongly influenced by the adjacent attractors' properties.**

***Index Terms*— Active Q-switching, chaos, GTWave fiber, jitter, laser dynamics, stimulated Brillouin scattering, Yb-doped fiber.**

I. Introduction

Q-SWITCHED Ytterbium doped fiber lasers (QS-YDFLs) producing energetic pulses in a nanosecond range are attractive sources of light for using in many practical areas such as laser marking and cutting [1], nonlinear frequency conversion [2], [3], supercontinuum generation [4]–[6], laser-initiated ignition [7], etc. The important features of such lasers are a long interaction length of the pump light with the active fiber core, permitting to reach a high fiber gain, and single transversal mode operation, important for technological applications.

It is frequently observed in actively and passively QS-YDFLs that output pulses have multi-peak structure with an interval between the adjacent sub-peaks being equal to the cavity round-trip time [8]–[10]. Such shape of Q-switching (QS) pulses is fully explained by the model of two contra-propagating waves that travel through a long fiber cavity [8], [11]–[14]. Another feature of QS-YDFLs is pulse jittering observed mostly in passively QS lasers [15], [16], which deteriorates the regime quality.

It is also known that in QS solid-state lasers, timing jitter is normally ruled by chaos [17]. Furthermore, the period doubling and deterministic chaos in the pulse energy distribution are observed in such lasers [18]. Recently, nonlinear dynamics of fiber lasers upon periodical modulation of intracavity loss (analog of active QS) was inspected theoretically [19] where a generalized multistability was shown to comprise the generation of QS pulses in multi-periodical and chaotic attractors. Despite a great number of researches that dealt with the dynamics of QS solid-state lasers exists, no comprehensive study – neither theoretical nor experimental – was made to date with fiber lasers.

The present paper serves to fill, at least partially, the gap. Below, we present a detailed experimental analysis of the dynamics of an actively QS (AQS) fiber laser built using an Yb-doped GTWave ("twin" or "dual") fiber [20]–[23]. Our aim was to make, on its example, a deeper insight into the details inherent in QS fiber lasers for getting a more complete picture of their nonlinear dynamics. We believe this would be important for further enhancement and optimization of fiber lasers of such kind.

In the laser under study, an AQS unit is a standard acousto-optical modulator (AOM) with fiber outputs, which provides fast change in the cavity Q-factor. The GTWave active fiber [20] was chosen as one of the best solutions for simplifying an overall laser implementation and, at the same time, for clarifying the physics that stands behind AQS regimes.

We demonstrate further that an AQS regime is mostly featured both by the AOM on/off repetition rate (f_m) and the AOM transparency window (or "gate"). If the AOM gate is fixed while f_m is increased from the lowest values, the laser consequentially passes through a set of regimes where QS pulses appear at the first, second and third sub-harmonics of the AOM repetition rate (so-called period-1 (P1), period-2 (P2), and period-3 (P3) attractors).

Depending on the attractors' numbers, the scenarios that may occur in the areas between the adjacent attractors upon

Manuscript received June 7, 2012; revised September 1, 2012; accepted September 18, 2012. Date of publication September 28, 2012; date of current version October 16, 2012. This work was supported in part by the Ministerio de Economía y Competitividad under Project TEC2008-05490 of Spain, the Generalitat Valenciana under Project PROMETEO/2009/077 of Spain, and "Omics Research Ltd." Hong Kong.

Y. O. Barmenkov and A. V. Kir'yanov are with the Centro de Investigaciones en Óptica, León 35150, Mexico (e-mail: yuri@cio.mx; kiryanov@cio.mx).

M. V. Andrés is with the Departamento de Física Aplicada ICMUV, Universidad de Valencia, Burjassot 46100, Spain (e-mail: miguel.andres@uv.es).

Color versions of one or more of the figures in this paper are available online at http://ieeexplore.ieee.org.

Digital Object Identifier 10.1109/JQE.2012.2220530

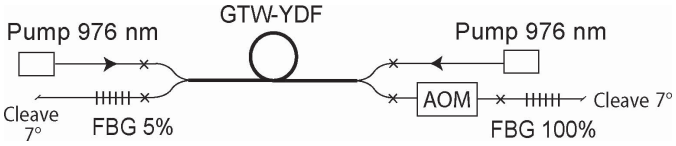

Fig. 1. AQS GTW-YDFL configuration. Crosses: fiber splices.

an f_m increase are either a smooth bifurcation route when amplitude/energy of each even QS pulse increases whilst that of each odd QS pulse decreases, or chaos. At the short AOM gates, the laser shows much richer dynamics as compared to the long ones. Furthermore, at very low f_m (<39 kHz), the laser turns to a stochastic pulsed operation, or "self-Q-switching" (SQS), initiated by the stimulated Brillouin scattering (SBS) process [8], [24], [25], which interferes with the "normal" AQS regime, given by the AOM's repetition rate f_m.

II. Experimental Setup

The experimental configuration of the AQS GTWave Yb doped fiber laser (GTW-YDFL) is shown in Fig. 1. The GTWave-Yb doped fiber (GTW-YDF) consists of two evanescently coupled fibers, one of them being multimode un-doped pump fiber with core diameter of 110 μm and the other – Yb doped (laser) fiber with core diameter of 11 μm, cut-off wavelength of 1.05 μm, and Yb^{3+} concentration of 8.5×10^{19} cm^{-3}. The outer diameters of both fibers forming the twin are 125 μm. The effective absorption of the pump light evanescently coupled from the pump to the laser fiber of the GTWave couple was measured to be 1.6 dB/m at 976 nm.

Two fiber-coupled 976-nm semiconductor lasers with maximal output powers of around 4.5 W each were used to pump the GTW-YDFL through the multimode pump fibers at both sides of the cavity. The length of the GTW-YDF was chosen to be 12.5 m, which provided effective pump absorption over the entire fiber length. In experiments, pump power was maintained at the maximum, 4.5 W $\times$ 2 = 9 W.

The laser cavity was formed by two fiber Bragg gratings (FBGs) with reflection coefficients of 5% (the laser output) and 100% (the rear cavity side), both centered at 1064 nm. The bandwidth of FBGs was around 100 pm and the total laser cavity length was 15.1 m.

The fiber-coupled AOM (M111-2G-F2S, *Gooch & Housego*) was placed between the laser fiber and 100%-FBG. The AOM operated at 1064 nm with a driving acoustical frequency of 111 MHz, the inserted loss was approximately 3 dB/pass and the AOM back reflection was nearby -35 dB.

The laser output was connected to an optical spectrum analyzer (OSA) or to a high-frequency photo-detector (with 1.2 GHz bandwidth) connected, in turn, to a fast digital oscilloscope (with 2.5 GHz bandwidth).

III. Experimental Results and Discussion

The experiments were fulfilled at the AOM repetition rates ranged from DC to 200 kHz and three values of the AOM gate: 1, 2, and 5 μs. It was found that, at low AOM repetition rates (DC to 38 kHz) and all the AOM gates, the QS regime is very different from the one at the higher repetition rates. Next we show that this one is established by the intra-cavity SBS process and thus is stochastic in nature, as being produced by noisy amplified spontaneous emission (ASE) and weak reflection from the AOM. Notice that the laser dynamics regimes to be featured below did not differ on either the AOM repetition rate was increased or decreased.

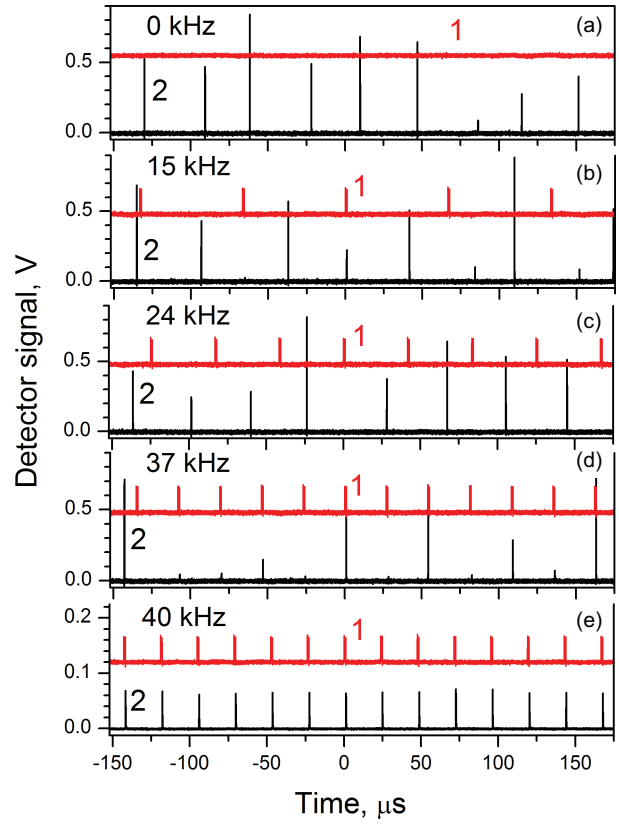

Fig. 2. Laser output signals obtained at different AOM repetition rates (a) 0 kHz, (b) 15 kHz, (c) 24 kHz, (d) 37 kHz, and (e) 40 kHz. In each snapshot, curves 1 (red) correspond to the control signal applied to the AOM driver and curves 2 (black) correspond to the laser signal.

A. SBS-Induced SQS

The SBS-induced self-QS regime (further – SQS) occurs in our experimental conditions at repetition rates $f_m < 39$ kHz (see Fig. 2 where oscilloscope traces are obtained for the AOM gate of 2 μs). Usually similar regimes are observed in Yb-doped fiber lasers with a very low Q-factor of the cavity (see e.g. [24]). Note that the total round-trip loss in our laser, when the AOM is blocked, is about 48 dB, which is produced by small reflections from 5%-FBG and from blocked AOM. This regime is characterized by short QS pulses with peak power of up to 3 kW and chaotic distributions of amplitude and intra-pulse spacing in the time domain. Pulse width (at a 3 dB level) was measured to be about 40 ns, the value quite different from the one observed at true AQS to be discussed further.

It is worth noticing that at f_m below 27 kHz, the SBS-induced SQS is the only pulsed mode observable in the GTW-YDFL whereas at f_m ranging from 27 kHz to 38 kHz

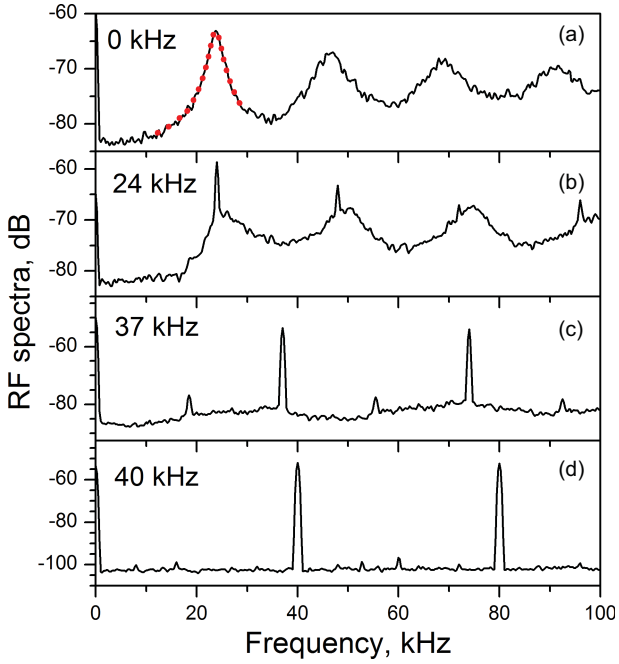

Fig. 3. RF spectra of QS pulses obtained at four different AOM repetition rates (a) 0 kHz, (b) 24 kHz, (c) 37 kHz, and (d) 40 kHz. Red dot curve in snapshot (a): fit by the Lorenzian function with a half-width of about 2 kHz.

a competition between the SQS and AQS modes occurs. It also deserves mentioning that at increasing the AOM repetition rate within this frequency range, the SBS-induced QS pulses become less and less probabilistic while the AQS pulses becomes more and more stable. The amplitude of AQS pulses ($f_m = 39$ kHz to 40 kHz) is approximately 13 times less than the amplitude of SBS-induced SQS pulses: Compare snapshots in Fig. 2(a) and Fig. 2(e).

The RF spectra of the laser signal are shown in Fig. 3. It is seen that, when the AOM is blocked (Fig. 3(a)), an average frequency of QS pulses is $f_0 = 23.7$ kHz and the shape of the RF spectrum resembles the one of relaxation fluctuations in continuous-wave lasers [26]. The first "relaxation" peak (see dash red curve in Fig. 3(a)) is well fitted by the Lorentzian function, which is the manifestation of the noisy (ASE) origin of the SBS-induced SQS.

At the AOM repetition rate $f_m = 24$ kHz, partial frequency locking is established in the system (see Fig. 2(c)) owing to virtual equality between f_m and f_0, which holds when a lone QS pulse is generated between each two adjacent AOM gates. This feature explains the appearance of narrow spectral peaks in the spectra; see Fig. 3(b). Since QS pulses are distributed chaotically by the amplitude and time separation, the narrow peaks appear above the noise pedestal, similar to the one shown in snapshot 3(a).

At the f_m values within a narrow spectral interval below the pure AQS threshold, frequency locking appears again ($f_m = 37$ kHz): pulses of both types, the SBS-induced SQS pulses (the biggest in amplitude) and the regular AQS ones (the smallest in amplitude) which are in-phase with the AOM gate, are seen to coexist (Fig. 2(d)). Because of the chaotic distribution of pulses by amplitude, the peaks in the

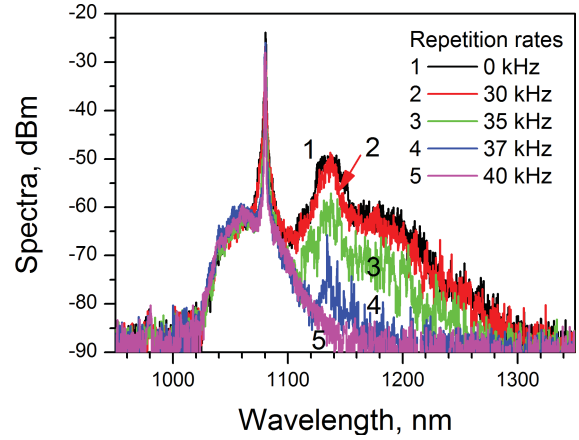

Fig. 4. Optical spectra of the laser measured at different AOM repetition rates (OSA resolution is 1 nm).

RF spectrum corresponding to this f_m are still seen on the noise pedestal (Fig. 3(c)) but they are much smaller than those observed at $f_m = 24$ kHz (Fig. 3(b)).

At the repetition rates $f_m \geq 39$ kHz the laser turns to pure AQS mode that is characterized by strong frequency locking and very low noise offset of the RF spectrum (see Fig. 2(e) and Fig. 3(d)). Some details of this regime, which occur at the higher repetition rates, will be featured below.

One more thing to be mentioned is a peculiar character of the transformations in optical spectra, which occur at increasing the AOM repetition rate; see Fig. 4. It is seen that, in a broad range of f_m (DC to 30 kHz), the optical spectrum changes insignificantly: compare black curve 1 with red curve 2 in Fig. 4. A sharp laser peak and several smooth Stokes peaks that correspond to the stimulated Raman scattering (SRS) process, gained by inversion in the Yb^{3+} system, are revealed to coexist.

At increasing f_m from 30 kHz, the Stokes peaks steadily decrease in magnitude until they disappear at all at $f_m \geq 39$ kHz, which is well understandable if to remember that the GTW-YDFL transients from SBS-induced SQS to pure AQS mode, with pulse amplitude in the latter being much less than in the former (see Fig. 2). In other words, such transformations in the optical spectra, rather swift indeed (compare curves 3 to 5 in Fig. 4), arise when the AQS pulse peak power becomes too small to reach the SRS threshold.

From curve 5 in Fig. 4 (which corresponds to almost regular AQS; see again Fig. 2(e) and Fig. 3(d)), we can estimate the ASE contribution: it is negligibly small ($< 2\%$) as compared with the total output power averaged over many QS cycles.

Note that very similar regimes are observed at other AOM gate values (1 μs and 5 μs).

B. Laser Dynamics at 5-μs AOM Gate

The laser dynamics observed at the AOM gate of 5 μs is simpler as compared to the shorter ones (see sub-sections *C* and *D*). Thus, we start an inspection of the QS features for this case.

Within an $f_m = 39$ kHz to 140 kHz range of the AOM repetition rates, the GTW-YDFL generates in a common

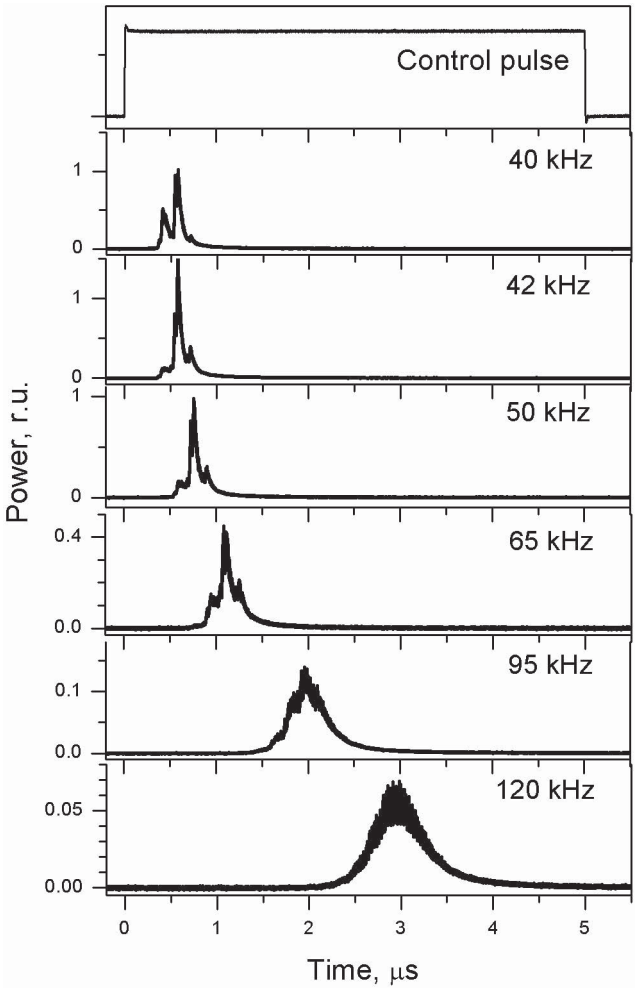

Fig. 5. Snapshots of QS pulses obtained at AOM gate of 5 μs and repetition rates from 40 to 120 kHz. The upper snapshot demonstrates a signal applied to the AOM driver. Here and in all figures below pulse power is normalized to the value of QS peak power measured at $f_m = 40$ kHz (180 W).

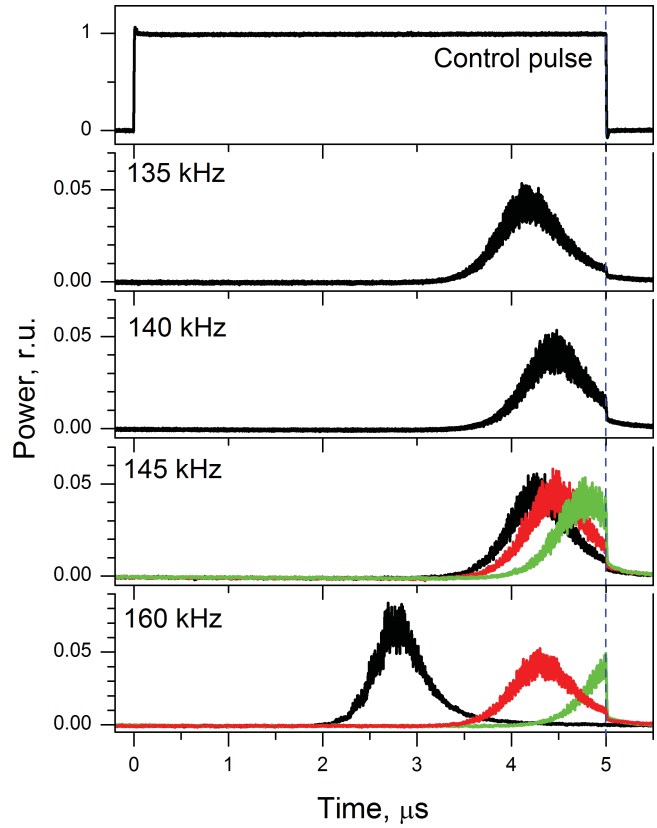

Fig. 6. Examples of the QS pulses measured at the AOM gate of 5 μs in the range of the AOM repetition rates from 135 to 160 kHz. The AOM repetition rates are indicated at the corresponding curves. Vertical dashed line: moment of the AOM switching off.

P1 attractor (a single stable pulse per AOM gate); see Fig. 5. The peak power of AQS pulses measured at $f_m = 40$ kHz is around 180 W. When the modulation frequency is increased from $f_m = 145$ kHz to 180 kHz, the laser turns to a chaotic regime. [We didn't study the laser at $f_m > 180$ kHz since at these frequencies the AOM duty cycle becomes nearby 100%, the value that makes instable the pulse generator used to control the AOM driver.]

One of interesting features to be mentioned here is that at not so high f_m the QS pulses are composed of two or three sub-pulses, depending on f_m value. Adjacent sub-pulses are always separated by ≈145 ns, the time that corresponds to the round-trip of light in the laser cavity, and a sub-pulse's width is ≈100 ns, with the total width of an overall QS pulse being ≈250 ns. At increasing f_m, the delay of QS pulse grows relatively to a moment of the AOM opening, while its energy is redistributed among the sub-pulses that compose it; see Fig. 5. At the same time the QS pulse amplitude and energy decrease, being a consequence of diminishing of population inversion in the Yb^{3+} system. At $f_m \sim 120$ kHz and higher, a QS pulse transforms to the Gaussian-like in shape and its overall width approaches ≈700 ns.

For better understanding, all the QS pulses shown in Fig. 5 (as well as the ones in all figures below) are shifted in the time domain by a certain value defined by cutting QS pulses off, which coincides with the time of the AOM switching off (as it is seen in Fig. 6). Thus, the real time delay of a QS pulse registered at 5%-FBG (the GTW-YDFL output) is equal to that indicated on the time axis, increased by 67 ns (it is the time interval corresponding to the optical path (14 m) from AOM to this FBG). Taking this into account, we find, for instance, that the first detectable sub-pulse of a QS pulse at $f_m = 40$ kHz arises after 2.5 round-trips relatively to the opening time of the AOM.

At f_m equal to 135 kHz or higher (see Fig. 6), QS pulses become broken by the AOM switching off process. If pulse energy is cut at the level of approximately 5–7%, the laser turns to chaotic oscillation with a random distribution of both the pulse delay and energy to arise and thus producing significant timing and amplitude jitters.

The examples of this behavior are presented by the snapshots recorded at $f_m = 145$ and 160 kHz, which are shown at the bottom of Fig. 6. The higher f_m the broader the range of pulse delay is. Most probably, this chaotic attractor is established in the laser due to the high QS duty cycle (also compare with a transitional regime to arise between the adjacent attractors P1 and P2 at the AOM gate of 2 μs, which is reported in the next sub-section).

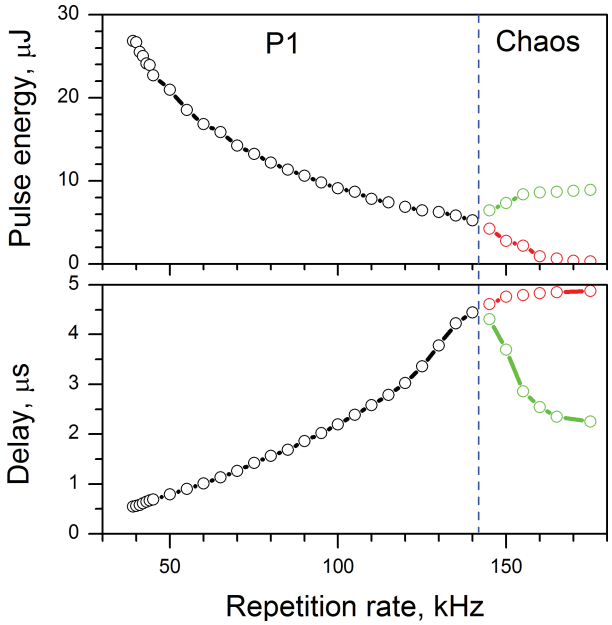

Fig. 7. Dependencies of QS pulse energy and delay on AOM repetition rates (the AOM gate is 5 μs).

The AQS regime reported above is resumed in Fig. 7 where we present the dependencies of both the pulse energy and pulse delay (measured as an interval between the moments of AOM opening and the pulse mass center) on modulation frequency f_m (bifurcation diagrams). It is seen that, within the range $f_m = 39$ kHz to 140 kHz (P1 attractor), pulse energy decreases by more than 5 times whereas pulse delay increases by more than 8 times. In the figure, the red and green curves on the right side from the dash line show the borders that limit the allowable variations of QS pulse energy (top) and delay (bottom). [Similar attributions are implied for all other chaotic regimes to be discussed further.]

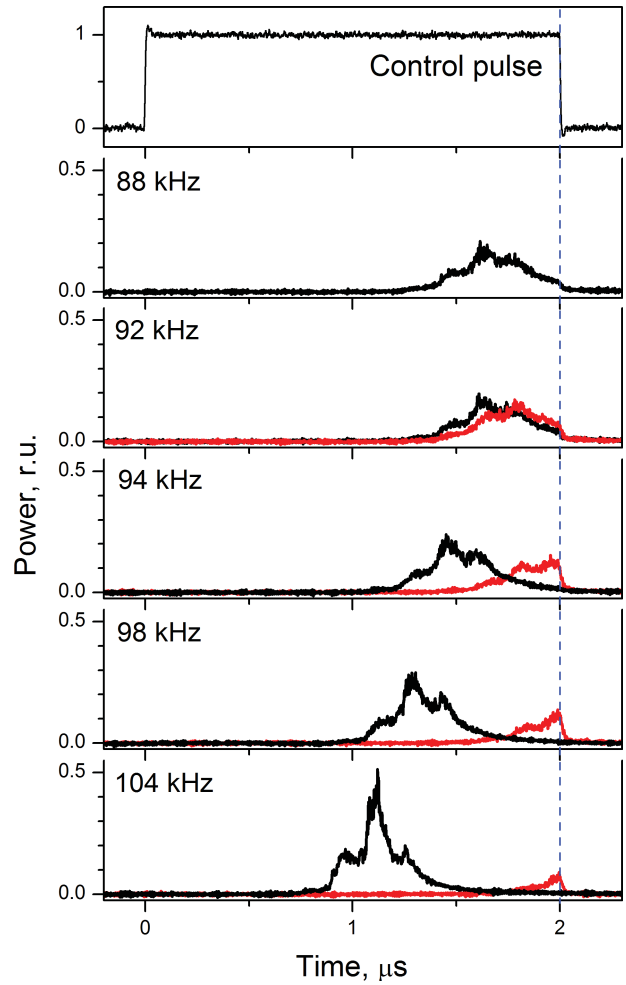

Fig. 8. Snapshots of QS pulses obtained at the AOM gate of 2 μs and repetition rates from 88 to 104 kHz. Vertical dashed line: moments of switching the AOM off.

C. Laser Dynamics at 2-μs AOM Gate

For the AOM gate of 2 μs and the range of $f_m = 39$ kHz to 90 kHz, the main feathers of QS pulses are very similar to the AOM gate of 5 μs, including the pulse shape, amplitude/energy, and delay. However the laser dynamics at the AOM gate of 2 μs is richer than that discussed above, which is associated with the fact that QS pulse cutoff occurs now at much lower AOM repetition rates than in the previous case. For example, with f_m growth, the transitional regime that arises at passing P1 attractor, starts now at $f_m = 92$ kHz (see Fig. 8), not at $f_m = 145$ kHz as at the AOM gate of 5 μs.

Also similarly, the bifurcation point appears when QS pulses are cut off by switching the AOM off (we again take this event to occur when pulse energy is cut off at the level of 5 to 7%). At this, each even pulse is characterized by growth in amplitude and energy and by drop of delay with f_m growth whereas the behavior of each odd pulse has an opposite character. An explanation for this is that a powerful pulse depopulates Yb^{3+} inversion down to a level at which the next pulse needs more time to get growing, which finally results in its full cutting off at the moments of switching the AOM off and *vice versa*.

With further growth of f_m, the odd pulses gradually disappear whereas the even ones steadily become effectively generated at a half of f_m: in this way P2 attractor is born.

Interestingly, no chaotic regime is observed in this transitional range of f_m. Furthermore, AOM pulses generated in the area of P2 attractor are very similar (in amplitude, energy, and shape), at a certain modulation frequency f_m^*, to the ones generated at a "half" frequency ($f_m^*/2$); see e.g. Fig. 9 – where f_m^* was chosen to be 130 kHz – and also compare the pulses in this figure with the one shown in Fig. 5, obtained at the repetition rate of 65 kHz.

At the frequencies $f_m = 184$ kHz and higher, the laser enters a new transitional regime that occurs between P2 and P3 attractors. At f_m ranged from 184 kHz to 200 kHz, alternating in the QS pulse amplitude and delay is observed, likely in the transitional regime shown in Fig. 8, with alone difference being that pulses with the same amplitude occur now at each four periods (not at each two) of a repetition rate: see Fig. 10 where we exemplify this feature for $f_m = 95$ kHz and 190 kHz.

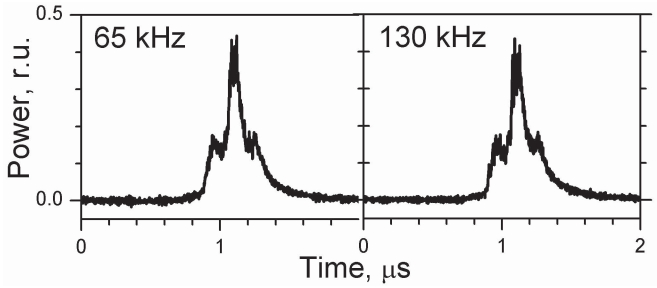

Fig. 9. Examples of AQS pulses obtained at repetition rates 65 (left) and 130 kHz (right). The AOM gate is 2 μs.

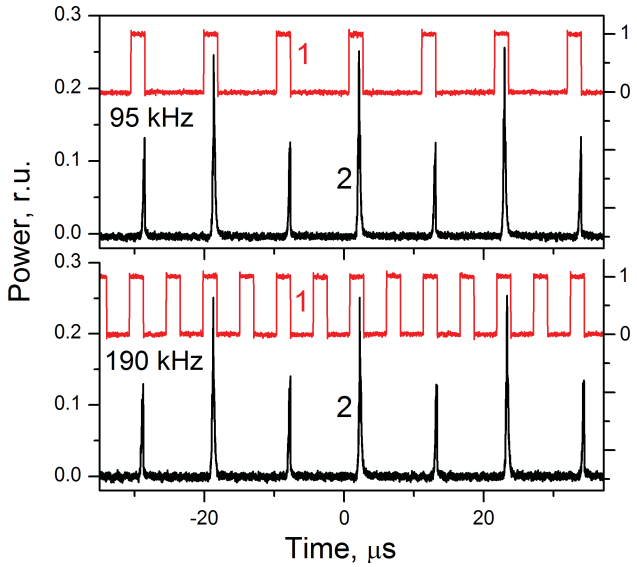

Fig. 10. Snapshots of QS pulses obtained at repetition rates 95 and 190 kHz. Right scale: curves 1 demonstrate the control signals. Left scale: curves 2 demonstrating the QS pulses. The AOM gate is 2 μs.

The AQS regimes observed at the AOM gate of 2 μs are resumed in Fig. 11. Generally, for f_m ranged from 39 kHz to 200 kHz, the two stable attractors, P1 and P2, and the two transitional regimes, TR1 and TR2, are observed. From here, one can see that for P1 and P2 attractors the slopes of pulse energy and delay *vs* repetition rate are correspondingly negative or positive (see solid lines that fit the experimental dependences) but differ by approximately two times, which is explained by the fact that QS pulses with the same energy need the same time to be released from the GTW-YDFL.

D. Laser Dynamics for AOM Gate of 1 μs

The laser dynamics observed at the AOM gate of 1 μs is the richest in the nonlinear dynamics appearance. We show below that in the range of the AOM repetition gates $f_m = 39$ kHz to 200 kHz the AQS pulsing occurs in three periodical attractors, P1, P2 and P3, with certain transients to happen between.

Generally, the overall behavior of QS pulses at 1-μs AOM gate is very similar to those observed at the longer gates, that is, the QS pulse amplitude and energy decrease while the pulse delay increases at increasing the repetition rate, within all the periodical attractors.

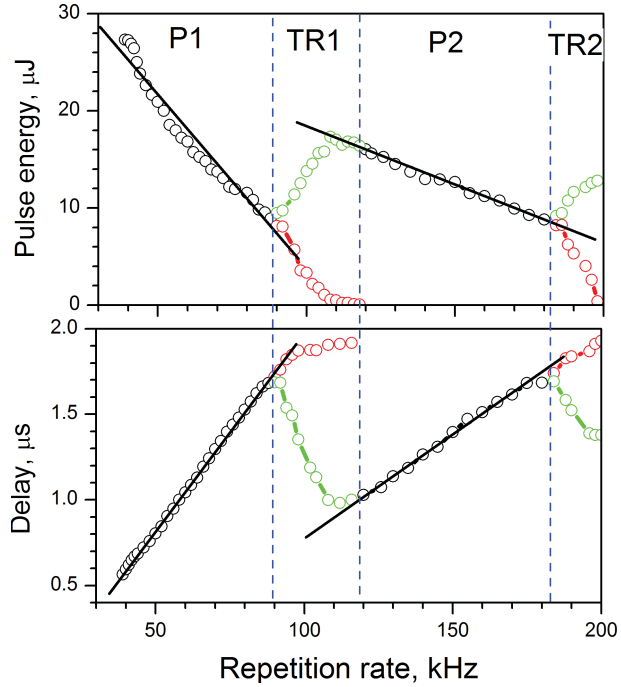

Fig. 11. Dependencies of QS pulse energy and delay AOM repetition rates. The areas labeled TR1 and TR2 mark the transitional areas between the adjacent attractors.

In P1 attractor, the behavior of the system is almost the same as in the cases discussed above (for the AOM gates of 5 and 2 μs); therefore we omit here its description. We only note that, at increasing the repetition rate upon 1-μs AOM gating, the GTW-YDFL enters a transitional regime that appears between P1 and P2 attractors by a slightly different manner. At f_m ranged from 58 kHz to 68 kHz, this regime is characterized by alternating in amplitude, energy, and delay of QS pulses: the higher f_m the difference between the adjacent pulses is stronger (see Fig. 12).

Within a narrow range, from 70 kHz to 72 kHz, i.e. just before P2 attractor's existence, the laser enters a chaotic oscillation (C1) that in our opinion originates from the presence of SBS-induced SQS pulsing, similar to the one discussed in sub-section *A* (see Fig. 13). Such a "giant" SQS pulse can be formed in the system after a small AQS pulse that has been generated within the previous AOM gate, which keeps a relatively high Yb^{3+} population inversion.

The irregular (stochastic) nature of the SBS-induced SQS pulsing in this case (see inset to Fig. 13) was already revealed by us in sub-section *A* and was also discussed in Ref. [8]. The most powerful SQS pulses are normally delayed by ≈330 ns (i.e. by a bit longer time than that corresponding to 2 round trips through the laser cavity). Note that this delay is less than delay of AQS pulses observed, say, at $f_m = 39$ kHz, the point from which stable pulses get arisen.

Worth noticing here is that, at longer AOM transparency gate (2 and 5 μs, see above), such a chaotic regime does not appear between P1 and P2 attractors.

Within a broad range of the AOM repetition rates ($f_m = 74$ to 112 kHz), the laser produces regular QS pulses in

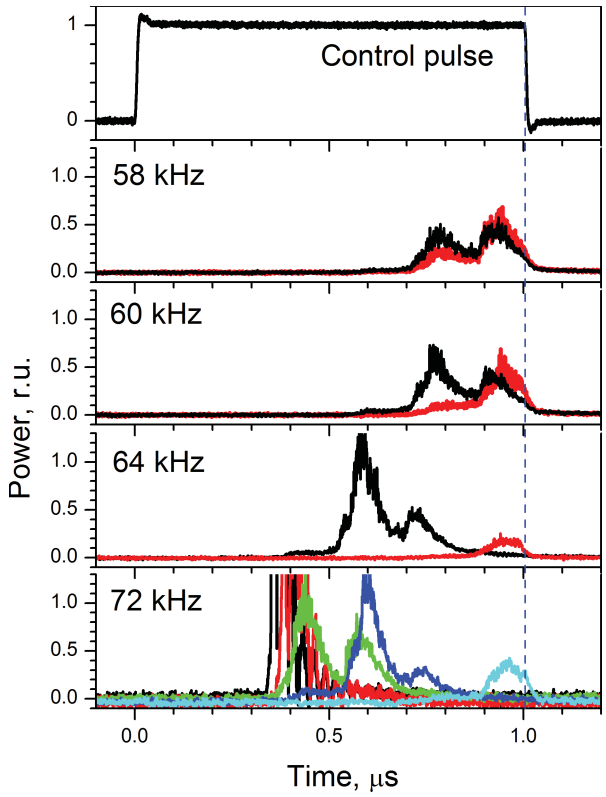

Fig. 12. Snapshots of QS pulses obtained at repetition rates from 58 to 72 kHz. Vertical dashed line: moments of switching the AOM off.

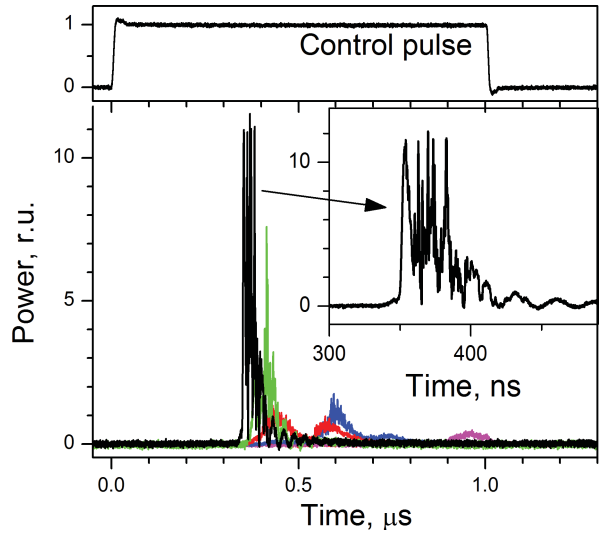

Fig. 13. Snapshots of SBS-induced SQS pulses captured at $f_m = 72$ kHz.

P2 attractor as it is seen in Fig. 14(a). Similarly to the cases discussed above, the pulses generated in this attractor, at a certain frequency, are very similar in the appearance to those generated at a half of the repetition rate, which occur in P1 attractor's area; compare Fig. 14(b) and Fig. 14(c). Thus, the GTW-YDFL operating in P2 attractor does not "see" each second gate of the AOM because its generation needs double time for effective "charging" of the active fiber.

The next transitional area at the AOM gate of 1 μs is observed between P2 and P3 attractors, i.e. at $f_m = 114$ kHz

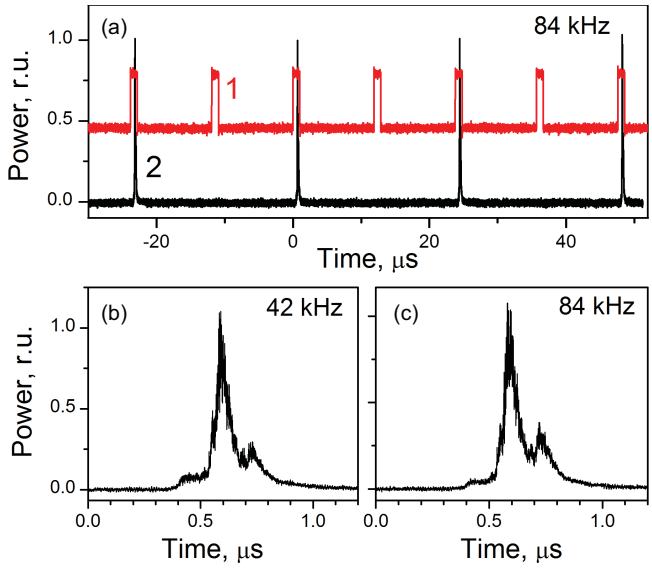

Fig. 14. Upper graph: Snapshots of QS pulses obtained at $f_m = 84$ kHz. (a) Signal 1 (red) corresponds to the AOM control pulses. Signal 2 (black) corresponds to the QS pulses. Lower graphs: examples of QS pulses obtained at (b) $f_m = 42$ kHz and (c) $f_m = 84$ kHz.

to 144 kHz; see Fig. 15. As well similarly to the case discussed above (see Fig. 12), at the beginning of this range, QS pulses are steadily split into two alternating but stable in amplitude pulses. Then, at $f_m = 132$ kHz to 144 kHz, the laser turns a new chaotic regime (C2).

Notice that origin of this chaotic regime is quite different from the one observed between P1 and P2 attractors (when SBS-induced SQS pulses having stochastic nature alter the regular operation of the laser). Instead, it appears as a result of intermittent instability given by the fact that the numbers of the adjacent attractors (P2 and P3) are not differ in a factor of two, which does not permit a smooth transformation from one attractor to the other.

Furthermore, at repetition rates from 145 kHz to 190 kHz, QS pulses are generated in P3 attractor where a single pulse per each three AOM gates (see Fig. 16) is born. At the larger repetition rates (at $f_m = 200$ kHz), the laser enters the transitional regime, also chaotic (C3), that arises between P3 and P4 attractors.

The overall dynamics of the GTW-YDFL at the AOM gate of 1 μs is summarized in Fig. 17. It is clearly seen from this figure that the AQS regime at 1-μs AQM gate is featured, in terms of pulse energy and delay, by the presence of the three stable attractors, P1, P2 and P3, and the three transitional areas, TR1, TR2 and TR3, in the whole range of repetition rates, i.e. from 39 kHz to 200 kHz.

Within all three transitional areas the chaotic regimes C1, C2, and C3 with different origins are observed, with C1 being associated with the presence of SBS-induced SQS and the other two, C2 and C3, being the appearance of cross-modulation between the adjacent P-attractors, i.e. being a general property of the GTW-YDFL nonlinear dynamics.

Interestingly, the slopes of the dependencies of pulse energy and delay upon f_m (see solid curves in Fig. 17, which fit the

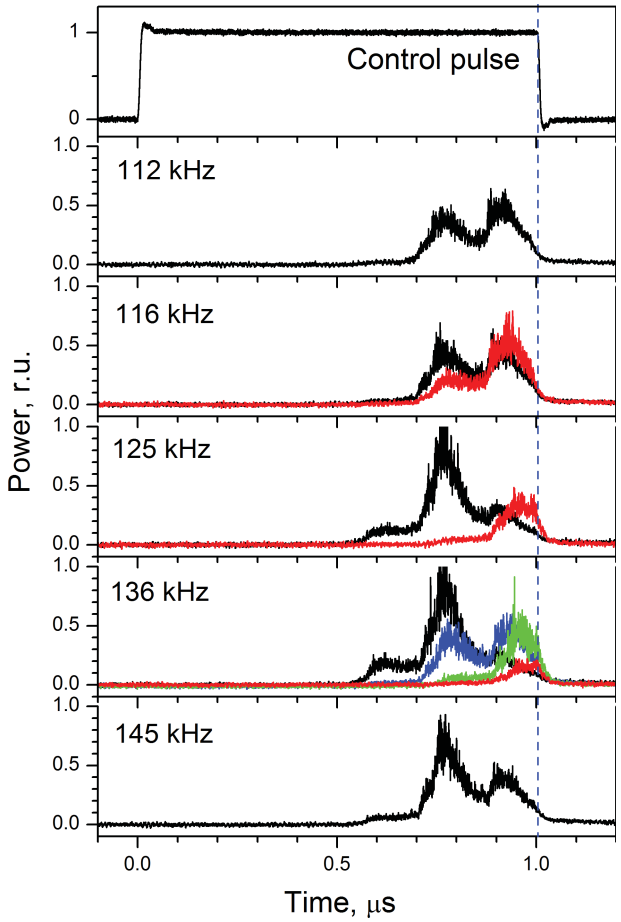

Fig. 15. Snapshots of AQS pulses obtained at repetition rates from 112 to 145 kHz.

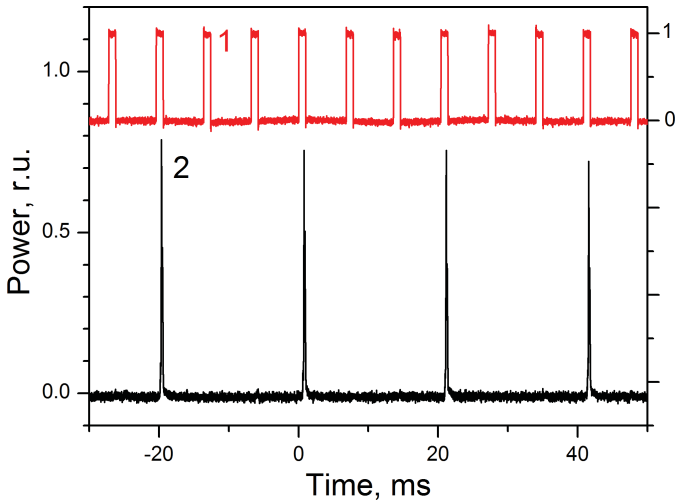

Fig. 16. Example of the QS pulses' train measured AOM repetition rate of 147 kHz. Right scale: Curve 1 is a trace of the AOM control signal. Left scale: curve 2 corresponds to QS pulses generated in P3 attractor. The AOM gate is 1 μs.

experimental results), which correspond to stable P1, P2, and P3 attractors, differ by the attractors' numbers. For example, P3 attractor has the slope approximately three times less than the one of P1 attractor, and so on. It is also worth noticing that

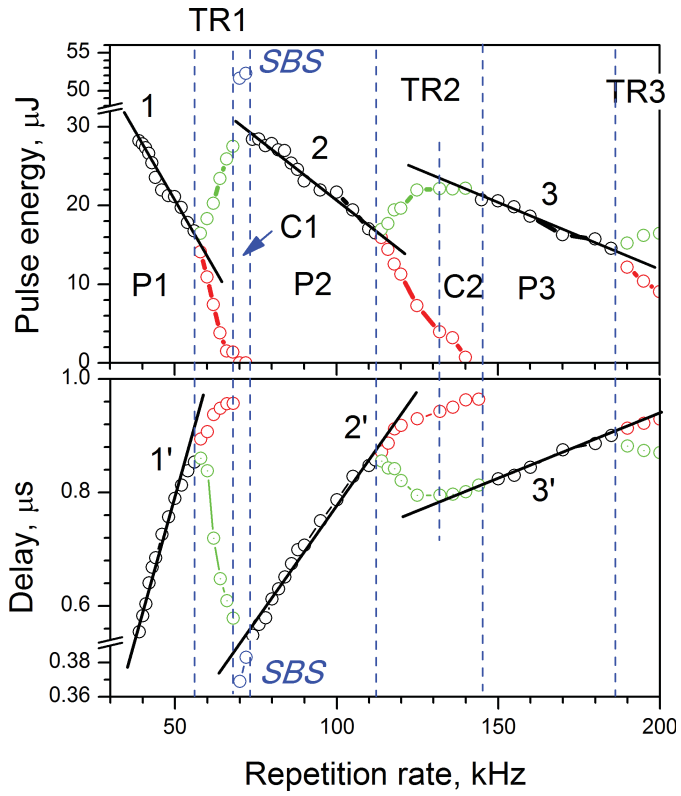

Fig. 17. Dependencies of pulse energy and delay on the AOM repetition rate (the AOM gate is 1 μs). The areas labeled TR1, TR2, and TR3 indicate the transitional regimes between the adjacent attractors P1, P2, P3, and P4. Points where SBS-SQS pulses arise are labeled SBS. Chaotic regimes are marked by C1 and C2 (chaotic regime C3 is not shown). The solid lines marked 1, 2, 3, and 1′, 2′, and 3′ fit the dependences of pulse energy and delay on repetition rate within P1, P2, and P3 attractors.

the energy, delay, and even shape of the QS pulses belonging to different attractors and taken at the repetition rates multiple to the attractors' numbers (f_m, $2f_m$, $3f_m$) are virtually the same; see Figs. 14 and 17.

One more fact deserves mentioning. As it is seen from Figs. 13 and 17, the energy of SQS (SBS-induced) pulses is by about two times bigger and their width is about five times less, as compared with regular (AQS) pulses; furthermore, the characteristic delay of these pulses is approximately two times less than delays of the regular AQS ones. Therefore, the SBS-induced SQS operation of the GTW-YDFL, although being stochastic and suffering from a strong jitter, is much more effective than the "classical" AQS regime.

IV. Conclusion

The present paper focuses on a detailed discussion of the dynamics of an actively Q-switched (AQS) fiber laser based on Yb-doped GTWave fiber where a Q-switch unit is based on a standard acousto-optical modulator (AOM) with fiber outputs. We explore the pulsed regimes that arise in the laser by varying the AOM parameters, namely, its repetition rate and gate width (i.e. its open state's window).

It is shown that the AQS regimes' appearance strongly depends on both these parameters. Generally, at the short AOM gates, the laser demonstrates a richer QS dynamics as

compared to the long ones. Furthermore, at the low repetition rates the laser turns to the regime of stimulated Brillouin scattering (SBS) induced self-Q-switching (SQS) that may interfere with the regular AQS operation at the higher repetition rates (a few kHz). At further increasing the AOM repetition rate, the laser passes through several regimes when AQS pulses are generated, depending on the AOM gate, i.e. either in common P1, P2, and P3 attractors, or in some peculiar transitional regimes that occur at the borders of these "regular" ones.

Depending on the attractors' numbers, the QS pulses arise at the first, second, or third sub-harmonics of the AOM repetition rates. In each attractor, the pulses consist of two or three subpulses at comparatively low repetition rates, but at the higher rates they tend to obtain a regular Gaussian-like shape. It is revealed that the shape, energy, and delay of the QS pulses belonging to different attractors and measured at the repetition rates multiple to the attractors' numbers are very close.

It is also found that various pulsed regimes are observed in the mentioned transients between the adjacent attractors. That is, a smooth bifurcation route may exist (when amplitude/energy of each even (odd) pulse increases (decreases)) but a chaotic circumstance may occur, too, strongly affected by amplitude and timing jitters. In turn, the chaotic regime may have different reasons: it may be either connected with the existence of SBS-induced SQS (and occurring in this case between P1 and P2 attractors at short AOM gates), or caused by the numbers of adjacent attractors (for instance, P2 and P3), not differing in a factor of two, or even arise when AOM duty cycle approaches 100%.

The results of the present work provide a continuous impetus to both fundamental and applied research in the field, which permits the reader to understand the physics of the QS Yb-doped fiber lasers deeper.

REFERENCES

[1] Y. Okamoto, R. Kitada, Y. Uno, and H. Doi, "Cutting of solid type molded composite materials by Q-switched fiber laser with high-performance nozzle," *J. Adv. Mech. Des. Syst. Manuf.*, vol. 2, no. 4, pp. 651–660, 2008.

[2] W. Shi, M. Leigh, J. Zong, and S. Jiang, "Single-frequency terahertz source pumped by Q-switched fiber lasers based on difference-frequency generation in GaSe crystal," *Opt. Lett.*, vol. 32, no. 8, pp. 949–951, 2007.

[3] W. Shi, M. A. Leigh, J. Zong, Z. Yao, D. T. Nguyen, A. Chavez-Pirson, and N. Peyghambarian, "High-power all-fiber-based narrow-linewidth single-mode fiber laser pulses in the C-band and frequency conversion to THz generation," *IEEE J. Sel. Topics Quantum Electron.*, vol. 15, no. 2, pp. 377–384, Mar. 2009.

[4] J. M. Dudley, G. Genty, and S. Coen, "Supercontinuum generation in photonic crystal fiber," *Rev. Modern Phys.*, vol. 78, no. 4, pp. 1135–1184, 2006.

[5] A. Roy, M. Laroche, P. Roy, P. Leproux, and J.-L. Auguste, "Q-switched Yb-doped nonlinear microstructured fiber laser for the emission of broadband spectrum," *Opt. Lett.*, vol. 32, no. 22, pp. 3299–3301, 2007.

[6] J. Cascante-Vindas, A. Diez, J. L. Cruz, and M. V. Andres, "Supercontinuum Q-switched Yb fiber laser using an intracavity microstructured fiber," *Opt. Lett.*, vol. 34, no. 23, pp. 3628–3630, 2009.

[7] J. Tauer, H. Kofler, and E. Wintner, "Laser-initiated ignition," *Laser Photon. Rev.*, vol. 4, no. 1, pp. 99–122, 2010.

[8] Y. Wang and C.-Q. Xu, "Actively Q-switched fiber lasers: Switching dynamics and nonlinear processes," *Prog. Quantum Electron.*, vol. 31, nos. 3–5, pp. 131–216, 2007.

[9] Y. Wang, A. Martinez-Rios, and H. Po, "Experimental study of stimulated Brillouin and Raman scatterings in a Q-switched cladding-pumped fiber laser," *Opt. Fiber Technol.*, vol. 10, no. 2, pp. 201–214, 2004.

[10] J. Y. Huang, H. C. Liang, K. W. Su, and Y. F. Chen, "High power passively Q-switched ytterbium fiber laser with Cr^{4+}:YAG as a saturable absorber," *Opt. Exp.*, vol. 15, no. 2, pp. 473–479, 2007.

[11] P. Roy and D. Pagnoux, "Analysis and optimization of a Q-switched erbium doped fiber laser working with a short rise time modulator," *Opt. Fiber Technol.*, vol. 2, no. 3, pp. 235–240, 1996.

[12] Y. Wang and C.-Q. Xu, "Switching-induced perturbation and influence on actively Q-switched fiber lasers," *IEEE J. Quantum Electron.*, vol. 40, no. 11, pp. 1583–1596, Nov. 2004.

[13] L. Pan, I. Utkin, and R. Fedosejevs, "Experiment and numerical modeling of high-power passively Q-switched ytterbium-doped double-clad fiber lasers," *IEEE J. Quantum Electron.*, vol. 46, no. 1, pp. 68–75, Jan. 2010.

[14] S. A. Kolpakov, Y. O. Barmenkov, A. D. Guzman-Chavez, A. V. Kir'yanov, J. L. Cruz, A. Díez, and M. V. Andrés, "Distributed model for actively Q-switched erbium-doped fiber lasers," *IEEE J. Quantum Electron.*, vol. 47, no. 7, pp. 928–934, Jul. 2011.

[15] J. Y. Huang, W. Z. Zhuang, W. C. Huang, K. W. Su, K. F. Huang, and Y. F. Chen, "Hybrid Q-switched Yb-doped fiber laser," *Opt. Exp.*, vol. 19, no. 10, pp. 9364–9370, May 2011.

[16] T. Hakulinen, R. Koskinen, and O. G. Okhotnikov, "Low jitter Q-switched fiber laser using optically driven surface-normal saturable absorber modulator," *Opt. Exp.*, vol. 16, no. 12, pp. 8720–8726, Jun. 2008.

[17] M. Kovalsky and A. Hnilo, "Chaos in the pulse spacing of passive Q-switched all-solid-state lasers," *Opt. Lett.*, vol. 35, no. 20, pp. 3490–3500, Oct. 2010.

[18] J. Dörring, A. Killi, U. Morgner, A. Lang, M. Lederer, and D. Kopf, "Period doubling and deterministic chaos in continuously pumped regenerative amplifiers," *Opt. Exp.*, vol. 12, no. 8, pp. 1759–1768, Apr. 2004.

[19] J. M. Saucedo-Solorio, A. N. Pisarchik, A. V. Kir'yanov, and V. Aboites, "Generalized multistability in a fiber laser with modulated losses," *J. Opt. Soc. Amer. B*, vol. 20, no. 3, pp. 490–496, Mar. 2003.

[20] A. B. Grudinin, D. N. Payne, P. W. Turner, L. J. A. Nilsson, M. N. Zervas, M. Ibsen, and M. K. Durkin, "Multi-fibre arrangements for high power fibre lasers and amplifiers," U.S. Patent N6 826 335, Nov. 30, 2004.

[21] D. A. Grukh, A. E. Levchenko, A. S. Kurkov, and V. M. Paramonov, "Self-Q-switched ytterbium-doped fibre laser with intracavity spectral conversion," *Quantum Electron.*, vol. 35, no. 5, pp. 442–444, 2005.

[22] S. M. Kobtsev, S. V. Kukarin, and Y. S. Fedotov, "High-energy Q-switched fiber laser based on the side-pumped active fiber," *Laser Phys.*, vol. 18, no. 11, pp. 1230–1233, 2008.

[23] A. V. Kir'yanov and N. N. Il'ichev, "Self-induced laser line sweeping in an ytterbium fiber laser with non-resonant Fabry–Pérot cavity," *Laser Phys. Lett.*, vol. 8, no. 4, pp. 305–312, Aug. 2011.

[24] S. V. Chernikov, Y. Zhu, J. R. Taylor, and V. P. Gapontsev, "Supercontinuum self-Q-switched ytterbium fiber laser," *Opt. Lett.*, vol. 22, no. 5, pp. 298–300, Mar. 1997.

[25] M. Salhi, A. Hideur, T. Chartier, M. Brunel, G. Martel, C. Ozkul, and F. Sanchez, "Evidence of Brillouin scattering in an ytterbium-doped double-clad fiber laser," *Opt. Lett.*, vol. 27, no. 15, pp. 1294–1296, Aug. 2002.

[26] A. E. Siegman, *Lasers*, Mill Valley, CA: Univ. Sci. Books, 1986, ch. 12.

Yuri O. Barmenkov (M'11) received the Ph.D. degree in radiophysics and electronics from Leningrad (St. Petersburg) State Technical University, Leningrad, Russia, in 1991.

He was a Assistant Professor and then a Senior Lecturer with the Department of Experimental Physics, St. Petersburg State Technical University, from 1991 to 1996. Since 1996, he has been a Research Professor with the Centro de Investigaciones en Optica, Leon, Mexico. He visited, for several periods, the Department of Applied Physics, University of Valencia, Valencia, Spain, as a Research Fellow, and the University of Joensuu, Joensuu, Finland, as a Visiting Scientist. He has authored or co-authored more than 130 scientific papers, and holds three patents. His current research interests include single-frequency, continuous wave and Q-switched fiber lasers, fiber optic sensors, and nonlinear optics of optical fibers.

Dr. Barmenkov is a National Researcher (SNI-III) in Mexico, and a Regular Member of the Mexican Academy of Sciences.

Alexander V. Kir'yanov (M'11) received the M.Sc. degree in optics and spectroscopy from M. V. Lomonosov Moscow State University, Moscow, Russia, and the Ph.D. degree in optics and laser physics from A. M. Prokhorov General Physics Institute, Russian Academy of Sciences, Moscow, in 1986 and 1995, respectively.

He was the A. M. Prokhorov General Physics Institute from 1987 to 1998. From 1989, he was a Visiting Scientist or a Lecturer with the Central Research Institute for Physics, Hungarian Academy of Sciences, Budapest, Hungary, the Institute of Material Chemistry, University of Technology, Tampere, Finland, the Imperial College, London, U.K., and the University of Valencia, Valencia, Spain. Since 1998, he has been a Research Professor with the Centro de Investigaciones en Optica, Leon, Mexico. He has authored or co-authored more than 160 scientific papers. His current research interests include solid-state and fiber lasers, and nonlinear optics of solid-state and optical fibers.

Dr. Kir'yanov is a National Researcher (SNI III) and a Regular Member of the Mexican Academy of Sciences.

Miguel V. Andrés (M'97) was born in Valencia, Spain, in 1957. He received the B.Sc. and Ph.D. degrees in physics from the University of Valencia, Valencia, in 1979 and 1985, respectively.

He was an Assistant Professor, a Lecturer, and a Professor with the Department of Applied Physics, University of Valencia, since 1983. He was a Post-Doctoral Researcher with the Department of Physics, University of Surrey, Surrey, U.K., from 1984 to 1987. He is the Founder of the Optical Fiber Laboratory Group at the University of Valencia and is responsible for the leadership and management of it. His current research interests include photonic crystal fibers, in-fiber acousto-optics, fiber lasers and new fiber-based light sources, fiber sensors, microwave photonics, and waveguide theory.